Adaptive Cross-Device Gait Recognition Using a Mobile Accelerometer

Thang Hoang*,**, Thuc Nguyen**, Chuyen Luong*, Son Do*
and Deokjai Choi*

Abstract—Mobile authentication/identification has grown into a priority issue nowadays because of its existing outdated mechanisms, such as PINs or passwords. In this paper, we introduce gait recognition by using a mobile accelerometer as not only effective but also as an implicit identification model. Unlike previous works, the gait recognition only performs well with a particular mobile specification (e.g., a fixed sampling rate). Our work focuses on constructing a unique adaptive mechanism that could be independently deployed with the specification of mobile devices. To do this, the impact of the sampling rate on the preprocessing steps, such as noise elimination, data segmentation, and feature extraction, is examined in depth.   Moreover, the degrees of agreement between the gait features that were extracted from two different mobiles, including both the Average Error Rate (AER) and Intra-class Correlation Coefficients (ICC), are assessed to evaluate the possibility of constructing a device-independent mechanism. We achieved the classification accuracy approximately 91.33 ± 0.67 % for both devices, which showed that it is feasible and reliable to construct adaptive cross-device gait recognition on a mobile phone.

Keywords—Gait Recognition, Mobile Security, Accelerometer, Pattern Recognition, Authentication, Identification, Signal Processing

1. INTRODUCTION

The explosion of mobility nowadays is setting a new standard for the information technology industry. Mobile device sales have skyrocketed over the recent years. Technology constantly evolves and creates more intelligent devices. Their abilities are not only limited to calling or texting, but also cover a variety of utilities, including portable storage and business applications, such as e-commerce or m-banking [2].

However, misconception of mobile devices as being an absolutely safe repository for storing critical information could cause owners to face up to security hassles. Such devices can be easily lost, stolen, or illegally accessed [1], which makes the sensitive and/or important information of mobile owners vulnerable (see more [1]). Consequently, identification settings have evolved to

Corresponding Author: Deokjai Choi

*   Department of Electronics and Computer Engineering, Chonnam National University, Gwangju, South Korea (hmthang2812@gmail.com, dchoi@jnu.ac.kr)
** DKE, Ho Chi Minh University of Science, Ho Chi Minh City, Vietnam

become more of a priority issue. The most widely used identification methods in mobiles are currently PINs, visual patterns, and passwords because of their ease in use and implementation. However, these methods are not always effective when considering remembrance and security aspects [1]. Implementations on a physiological biometric could completely overcome this issue [3]. However, it is hard to deploy them on mobile phones since existing mobile resources cannot guarantee the acquisition of specialized data, such as iris, fingerprints, etc., properly. Moreover, all these forced us to pay attention and perform explicit gestures that need to be captured (e.g., typing passphrases, facing to the front camera, etc.). This causes obtrusiveness and inconvenience in frequent use.

Thus, a friendlier yet more reliable identification mechanism, which can operate implicitly without users' awareness, needs to be discovered and aimed at ameliorating mobile security. Recently, a novel approach using wearable sensors to authenticate the human gait has been introduced and it has achieved potential results [11, 13]. Sensors are attached to the human body in various places such as the pocket, on the waist, and around footwear to record physical locomotion. This approach leads to takes advantage of modern mobile devices' sensing capabilities including GPS, accelerometer, magnetometer, gyroscope sensor, etc. Moreover, devices are usually put in its owners' pockets for most of the day [1], so acquiring walking signals can authenticate the gaits of people implicitly and continuously. For this reason, sensor-based gait identification has a significant advantage in being implemented in mobiles. It will provide developers with an edge over improving various techniques in identification.

Since 2009, this study has been initiated on mobiles and has achieved encouraging results [18, 19]. However, this type of mechanism has only been studied and has thus far only been proven to perform well on a certain device with a particular specification. There has been no research on establishing a device-independent model. Nowadays, the lifecycle of a mobile phone is eventually decreased. This is due to its evolution. Users are willing to change or upgrade their phone frequently after using it for a short amount of time. The gait identification mechanism should dynamically adapt with this tendency.

In this paper, we conduct a thorough examination on the impact of sensor quality on the gait recognition model. Using a pair of old-fashioned and modern mobile phones, which have different sampling rates for the built-in accelerometer, we collect gait signals simultaneously. Then, we measure the degrees of agreement between the gait features that have been extracted from signals acquired by such devices. Furthermore, various sampling rates are also analyzed to select an appropriate unique value for building a device-independent recognition model. With the results achieved from our experiment, our main contribution is that we are proposing a novel cross-device gait recognition with the accuracy rate of approximately 91.33%. The rest of this paper is organized into 4 sections. Section 2 presents related works. Section 3 presents our proposed recognition model. Section 4 summarizes the result from our experiments. Our conclusions are then presented in Section 5.

2. RELATED WORKS

Human gait has been considered to be a particular style and manner of how the human feet move and hence it contains information related to identity. In more explicit detail, the mechanism of the human gait involves synchronization between the skeletal, neurological, and muscu-

lar system of the human body [4]. In 2005, H. Ailisto et al. were the first to propose gait authentication[1] using wearable sensors [13] and Gafurov et al. [10] further expanded this area. In general, sensors are attached to various positions on the human body to record locomotion signals. Various sensors have been experimented with, including the gyroscope and the rotation sensor, but the acceleration sensor (or accelerometer in short) is the most commonly used. In this used one. There are two typical approaches: (1) Template Matching (TM) and (2) Machine Learning (ML). In (1), the acquired signal is preprocessed and then split into patterns. The best patterns that match the most characteristics of the subject are considered to be the representative gait templates. They are then stored as referred templates that correspond to the individual. Various distance metrics, such as Dynamic Time Warping (DTW) [9, 19, 14], Euclidean distance [8, 9], auto–correlation [13], and nearest neighbors [11] are used for calculating the similarity score between a given pattern and the referred templates.

The ML method is the most popular approach that is used in pattern recognition areas. In this approach, the gait signal is segmented into patterns. For each pattern, features are extracted in time domain, frequency domain, and wavelet domain, or by special techniques such as time delay embedding [18]. Extracted feature vectors are then classified using supervised classifiers like HMM [16], SVM [14, 15, 17, 18, 20], and ANN [5], LDA [5]. Some other works propose hybrid approaches in which either distance metrics, such as DTW [7] and Euclidean [10, 12] are used to measure the similarity scores of features that have been extracted in time and frequency domains, or where the similarity scores of gait templates can be considered as features that are used for classification [6].

In the early stages, most of the works that have used standalone sensors (SSs) have been implemented with a variety of success rates. However, they still have some restrictions. For example, SSs are relatively expensive, hard to attach because of their size, and the interface of some special sensors needs to be developed separately. Recently, the development of micro electro mechanical (MEMs) technology helped such sensors to be miniaturized and integrated inside mobile devices (known as mobile sensors – MS). Gait identification has been initially experimented on MS recently. In 2009, S. Sprager et al. used built-in accelerometer in Nokia cellphone positioned at the hip to collect and analyze gait signal [20]. Feature vectors for classification were built based on collected data using dimension reduction on cumulants by Principal Component Analysis (PCA). The classification in this module was accomplished by Support Vector Machines (SVM). They achieved about 90.3% accuracy. However, the number of experimental participants is rather small (6 persons). In comparison to SSs, MSs are designed to be cheaper and simpler to be embedded in mobile devices, and as a result the quality is not as guaranteed as with SSs. For example, the sampling rate is low and unstable, and the noise is rather high. Derawi et al. [19] showed that impact by redoing Holien's work [21] using MS instead of SS and achieved an EER of 20.1%, as compared to 12.9%. Table 1 summarizes the gait recognition approaches and their performances with various evaluation metrics, such as the Equal Error Rate (EER), Recoginition Rate (RR), etc. on both SS and MS.

---

1 The difference between authentication and identification is that authentication performs binary classification tasks, while identification performs multi-class tasks

Table 1. Gait recoginition systems using the Standalone (S) and Mobile sensors (M) ,including the Accelerometer (A) and Rotation Sensor (R) by the following methods: Template Matching (TM), Machine Learning (ML), and Hybrid (H)

Previous Work	Sensor / Sampling rate	Location	Method	No. of Subjects	Result
[14]	M–A / 27Hz	T Pocket	TM, ML	11	79.1%, 92.7% RR
[6]	S–A / 50Hz	Ankle	H	22 (16M 6F)	3.03% EER
[5]	9 S–R	Body	ML (LDA)	30 (25M 5F)	~ 100% RR
[15]	M–A	T Pocket	ML (SVM)	36	HTER: 10.1%
[7]	S–A / 40Hz	Ankle	H	22	3.27% EER
[16-17]	M–A / 120Hz M–A / 45Hz	Hip	ML (HMM) ML (SVM)	48 (30M 18F)	6.15% EER, 5.9% FMR, 6.3%FNMR
[8]	S–A / 100Hz	Ankle	TM (Euclidean)	10	20% EER
[18]	M–A / 25 Hz	T Pocket	ML (SVM)	25	100% RR
[9]	S–A / 100Hz	Hip	TM (PCA)	60(43M 17F)	1.6% EER
[19]	M–A / 45Hz	Hip	TM (DTW)	51 (41M 10F)	20% EER
[20]	M–A / 37Hz	Hip	ML (SVM)	6	90.3 ± 3.2% RR
[10]	S–A / 16Hz, 100Hz	Ankle Pocket Arm Hip	H (Euclidean) H (Manhattan)	21 (12M 9F) 100 (70M 30F) 50(33M 17F) 30 (23M 7 F)	5% EER 7% EER 10% EER 13% EER
[11]	S–A / 100Hz	Body	TM(NN)	30	96.7% RR
[12] [13]	S–A / 256Hz	Waist	TM(cross-corr.), H (FFT, histogram)	36 (19M 17F)	6.4 %, 10%, 19% EER

3. METHODOLOGY

3.1 Data collection

The Google Android HTC Nexus One and the LG Optimus G (Figure 1 [a, b]), were used to collect data. To make sure that the gait signals are acquired simultaneously with the most accurate rate on both devices, we roped them to be stuck together, as illustrated in Figure 1(c). The specifications of the two devices are described in Table 2. The sampling rates of the built-in accelerometers were set to the highest level of approximately 27 Hz, 100Hz, for the Nexus One and Optimus G mobile phones, respectively. The SENSOR_DELAY_FASTEST mode on the Android SDK was used to do this.

An application that controls the data acquisition process via Bluetooth communication is also designed to ensure that gait signals are collected simultaneously from both devices. A total of 14 volunteers, including 10 males and 4 females, with the average age ranging from 23 to 28, participated in our data collection.

The devices were put inside the subject's trouser pocket with a constant orientation, as shown in Figure 1(d). Since mobile devices are usually put freely in the trouser pocket, a misplacement error could occur. From our observation, adapting an effective wavelet decomposition algorithm could eliminate such an error. This algorithm will be discussed in Section 3.2.2. Each volunteer was asked to walk 12 laps at a natural pace on the ground. Each lap cost around 36 seconds. In total, we accumulated around 12 (laps) × 36 (seconds) × 14 (volunteers) = 6,048 seconds of walking time. Within the counting time, the acceleration forces acting on the phones were meas-

Table 2. Specifications of the Google Nexus One and the LG Optimus G

	HTC Google Nexus One	**LG Optimus G**
CPU	1 GHz Scorpion	Quad-core 1.5 GHz Krait
Memory	RAM 512Mb + 2GB SD Card	RAM 2GB + 16 GB internal storage
Sensor	BMA-150 Accelerometer	LG Accelerometer
Sampling rate	27 Hz (FASTEST MODE) Range: ± 2g	100 Hz (FASTEST MODE) Range: ± 4g
OS	Android 2.3.6	Android 4.1.2

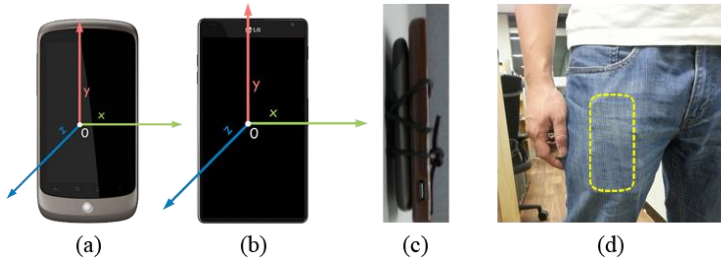(a)   (b)   (c)   (d)

Fig. 1. (a) Google Nexus One, (b) LG Optimus G, (c) Two devices are bound together to collect gait signals at the same time, (d) Both devices are put inside a trouser pocket

ured in three spatial dimensions (*X*, *Y*, and *Z* as illustrated in Figure 1[a, b]). Based on the relationships between gravity, acceleration, and motion, we present the output of the accelerometer as 3-component vectors as follows:

$$A = [a_X, a_Y, a_Z] \tag{1}$$

where a_X, a_Y, a_Z represents the magnitude of the acceleration forces acting on three directions, respectively.

3.2 Data pre-processing

3.2.1 Time interpolation

A mobile accelerometer works power saving mode. Its sampling rate is not stable and depends entirely on the mobile OS. The time interval between the two consecutive returned samples is not a constant. The sensor generates the value only when the forces acting on each dimension have a significant change. Hence, we applied a linear interpolation to the acquired signals to make sure that the time interval between two consecutive samples remained constant. The linear interpolation is calculated by:

$$s' = s_0 + \frac{(s_1 - s_0)(t' - t_0)}{t_1 - t_0} \tag{2}$$

where s_o, s_1 represents two samples collected at times t_o and t_1, respectively, (s', t') is the new generated point that lies between (s_0, t_0) and (s_1, t_1).

3.2.2 Noise elimination

When the accelerometer samples movement data from the user walking, some noises will inevitably be collected. These additional noises come from various sources (e.g., idle orientation shifts, screen taps, bumps on the road while walking). Moreover, the mobile accelerometer produces numerous noises as compared to standalone sensors, since its functionalities are fully governed by the mobile OS layer. A digital filter needs to be designed to eliminate noises and to concurrently reduce the impact of misplacement error.

We found that the multi-level wavelet decomposition and reconstruction method are significantly effective in eliminating noises. According to Figure 2, the input signal *S(n)* is decomposed into two equal parts, including the detail and coarse components. It uses a high-pass filter *(HF)* and low-pass filter (*LF*), respectively. Only coarse components are important for representing the characteristics of the signal so that the detail components are often eliminated to remove worthless information.

When the phone is put in the subject's trouser pocket, it rests near his/her thigh and as a result, a misplacement error could occur. From our observations, walking is a slow activity with a moderate fluctuation. Consequently, any strong acceleration is likely to last no longer than a few tenths of a second. Furthermore, once the phone is placed close to a joint of the leg, output signals are dominated by gravitational signals [22]. Hence, we use the Daubechies orthogonal wavelet with the order 6 being set at level *n* to eliminate noises and to concurrently reduce the influence of misplacement error. The value of *n* depends on the sampling rate of the recording devices. In our study, since experimental mobile phones are used with different sampling rates, *n* is selected as 2 then 3 for a sampling rate of 27Hz and 100Hz, respectively.
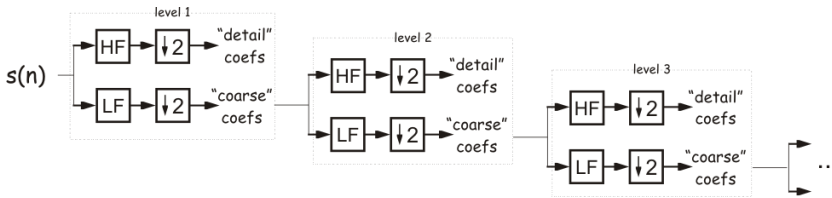

Fig. 2. Multi-level wavelet decomposition

3.2.3 Data segmentation

After noise has been removed, the signal is segmented into separated patterns. As already stated, gait recognition is based on the walking style of individuals. Meanwhile, walking is a cyclical activity. The acquired signal should be segmented according to gait cycles instead of according to a fixed interval (e.g., 5 or 10 seconds) as was done in previous works [15-17].

The gait cycle is defined as the time interval between two successive occurrences of one of the repetitive events when walking [23]. In other words, two consecutive steps form a gait cycle. As shown in Figure 3, the cycle starts with the initial contact of the right heel, and then it will continue until the right heel contacts the ground again. The left heel goes through exactly the same series of events as the right, but is displaced in time by half a cycle.

We designed an algorithm to detect gait cycle events that appear in the signal. At the time that the subject's right heel touches the ground, the association between the ground reaction force and inertial force together makes the *Y*-axis signal change strongly and to form negative peaks
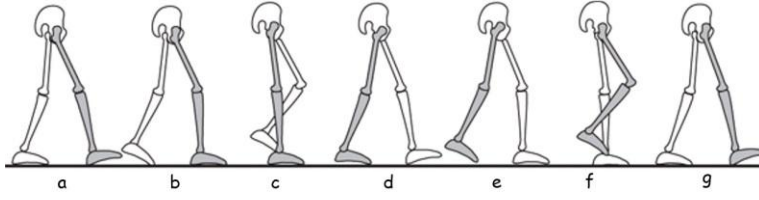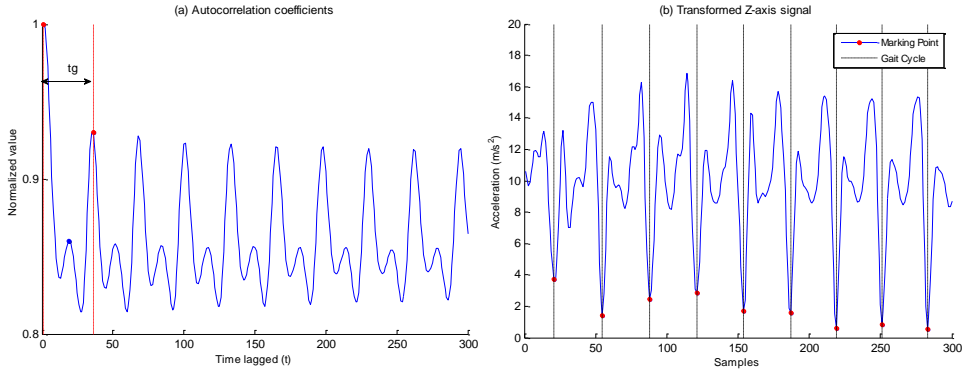
Fig. 3. Illustration of a gait cycle

Fig. 4. (a) Auto-correlation coefficients with the estimated tg (b) The detected marking points in the Z-signal

with absolute high magnitudes. These peaks are considered to be marking points, which are used to distinguish separated gait cycles (Figure 4[b]). A threshold that is calculated from the mean and standard deviation of the peak[2] set filters these high magnitude peaks. Moreover, the time gap tg between two gait cycles is also estimated to obtain the most precise set of marking points. tg is dynamically calculated based on each characteristic of the gait signal.

First, the autocorrelation algorithm is applied to the transformed Z-axis data to determine the regularity of the signal. Let A_m be the autocorrelation coefficient which is computed as:

$$A_m = \sum_{i=1}^{N-|m|} x_i x_{i+m} \tag{3}$$

where x_i is the time series data point, x_{i+m} is the time-lagged replication of x_i.

Then A_m is normalized to $[0,1]$ by dividing to A_0.

$$A_m = \frac{A_m}{A_0} \text{ with } A_0 = \sum_{i=1}^{N} x_i^2 \tag{4}$$

Figure 4(a) illustrates the autocorrelation coefficients A that represent the regularity of the

---

2 A point is called a "peak" if its value is greater (or lower in a negative peak case) than its predecessor and successor

walking signal. In this figure, the distance of two red peaks, in which the first one corresponds with A_0 and the other is denoted as A_k, determines the approximate time gap tg of gait cycles:

$$tg = t(A_k) \tag{5}$$

where $t(i)$ is the time-lagged of point i.

From our study, the gait signal is segmented into separated patterns in which each pattern contains *n=4* consecutive gait cycles and overlaps *n/2* gait cycles from the previous one. Features are extracted from every separated pattern in both time and frequency domains to obtain feature vectors, which are used as the input of classification tasks.

3.3 Feature extraction and classification

3.3.1 Time domain features

• Average maximum acceleration
$$\text{avg\_max} = \text{mean}(\max(GC_i))_{i=0}^{n-1} \tag{6}$$

• Average minimum acceleration
$$\text{avg\_min} = \text{mean}(\min(GC_i))_{i=0}^{n-1} \tag{8}$$

• Average absolute difference
$$\text{avg\_abs\_diff} = \sum_{i=1}^{N} |x_i - \bar{x}| \tag{9}$$

• Root mean square
$$\text{RMS} = \frac{1}{N} \sum_{i=1}^{N} x_i^2 \tag{11}$$

• 10-bin histogram distribution
$$\text{hist\_dist} = \langle n_j \rangle_0^9 \text{ with } n_j = \frac{\sum_i x_i}{\text{size}(bin_j)} \tag{7}$$

$$\frac{j(max - min)}{10} \le x_i \in bin_j < \frac{(j+1)(max-min)}{10}$$

• Standard deviation
$$\sigma = \sqrt{\left(\frac{1}{N-1}\right) \sum_{i=1}^{N} (x_i - \bar{x})} \tag{10}$$

• Waveform length
$$\text{wl} = \sum_{i=1}^{N-1} |x_{i+1} - x_i| \tag{12}$$

where x_i is the data point in time series of a segment, n is the number of gait cycles GC in the segment, and N is the number of data points in the segment.

These above features are extracted on 4 types of signal including the separating *X*, *Y*, *Z*-axis signal a_X, a_Y, a_Z and the magnitude $M = \sqrt{a_X^2 + a_Y^2 + a_Z^2}$.

• Time of a gait cycle
$$T_{\text{cad}} = \frac{\sum_i^n t(GC_i)}{n} \tag{13}$$

• Gait cycle frequency
$$f_{\text{cad}} = \frac{n}{\sum_i^n t(GC_i)} \tag{14}$$

where $t(GC_i)$ is the time length of gait cycle *i*.

3.3.2 Frequency domain features

• The first 40 FFT coefficients

$$fft = \langle X_k \rangle_{k=0}^{39} , X_k = \sum_{n=0}^{N-1} x(n)e^{-\frac{j2\pi kn}{N}} \tag{15}$$

• The first 40 DCT coefficients

$$dct = \langle X_k \rangle_{k=0}^{39} , X_k = \frac{1}{2}x_0 + \sum_{n=1}^{N-1} x_n \cos\left[\frac{\pi}{N}n\left(k + \frac{1}{2}\right)\right] \tag{16}$$

Similar to features in time domains, these coefficients are extracted on a_X, a_Y, a_Z, and M.

Note that the walking speed of users is not absolutely constant. Hence, the length of the gait cycles is not stable. Calculating coefficients in a frequency domain (e.g., FFT, DCT) requires window frames (or patterns) that have the same fixed length. Meanwhile, the length of the gait cycles fluctuates slightly around time gap tg. As a result, the number of data points in every gait cycle needs to be normalized by using our proposed algorithm [14] to make sure that frequency coefficients are calculated exactly. Lastly, the final feature vector, which is formed by all of the features that has been extracted in both time and frequency domains, is classified by using the Support Vector Machine.

3.4 Validating features extracted from both devices

In order to validate the feasibility of constructing a cross-device gait recognition model, the Average Error Rate (AER) [25] and Intra-class Correlation Coefficients (ICC) [26] are adapted to measure the level of agreement between concurrent gait features extracted from both mobile phones with different sampling rates of 32 Hz and 100 Hz. As illustrated in [27], ICCs value of < 0.4, 0.40 to 0.75, and > 0.75 are interpreted to represent poor, fair-to-good, and excellent consistency between the two measurements. The AER is calculated by:

$$AER = \frac{\sum_{id=1}^{M} \frac{\left|F_{A_{id}} - F_{B_{id}}\right|}{\left|F_{A_{id}}\right|}}{M} \tag{17}$$

The ICC is calculated by:

$$ICC = \frac{\sum_{id=1}^{M}\left|F_{A_{id}} - \mu\right|\left|F_{B_{id}} - \mu\right|}{Ms^2} \tag{18}$$

where:

$$\mu = \sum_{id=1}^{M} \frac{F_{A_{id}} + F_{B_{id}}}{2M} \tag{19}$$

$$s^2 = \sum_{id=1}^{M} \frac{\left(F_{A_{id}} - \mu\right)^2 + \left(F_{B_{id}} - \mu\right)^2}{2M} \tag{20}$$

with F_{T_k} being the feature of the kth subject, which is extracted from the signal acquired by device T.

3.5 The downsampling and upsampling rates of mobile devices

To measure the impact of the sampling rate on a recognition mechanism, gait signals acquired by the Google Nexus One and LG Optimus G (100 Hz) mobile phones were down/up-sampled to lower/ higher rates, which have been calculated by:

$$\text{sampling rate} = \{16 + 4k\} \text{ with } k = 1, 2 \dots, 21 \tag{21}$$

The linear interpolation illustrated in 3.2.1 is adapted as a method to down/up-sample. By looking at the classification results achieved from various sampling rates, we come to choose the only one value which gives the best classification accuracy as a standard value. Signals acquired from diverse sampling rates will be down/up-sampled to be equal to this value before performing preprocessing steps such as noise elimination, segmentation, feature extraction and classification.

4. RESULTS

4.1 The overall classification of both devices with their default settings

1,054 samples were extracted from our own dataset in total. This dataset was divided into two equal parts including *T-PART* and *P-PART*, which would be used for training and prediction, respectively. The number of collected samples corresponding to each volunteer is illustrated as shown in Table 3. We used Libsvm[3] [24] as the effective tool to perform the Support Vector Machine (SVM) classifier with the Radial Basis Function (RBF) kernel. Once using the RBF kernel, parameters including (γ, *C*) are very sensitive to the classification rate of this type of classifier. Hence, a 10-fold cross validation is also applied to the entire *T-PART* to deal with the issue of over fitting and finding an optimal pair (γ', *C'*). We achieved a cross validation accuracy rate of 100% at (γ', *C'*) = ($2^{-5.25}$, $2^{3.5}$). After that, all of the *T-PART* is trained again using this (γ', *C'*) to gain the final classification model that is used to predict *P-PART*. We achieved the classification accuracy of 99.81% (1052/1054) and 97.53% (1028/1054), which correspond to the gait signals acquired by the Google Nexus One and LG Optimus G phones, respectively. The confusion matrices of two cases are illustrated in Figure 5.

Upon our examining the results achieved from the data collected by both devices, we were able to determine that the classification rate of Google Nexus One is slightly better than LG Optimus G and that regardless of the sampling rate of the built-in accelerometer, the LG Opti-

---

3 Software available at http://www.csie.ntu.edu.tw/~cjlin/libsvm

Table 3. The number of samples used for training and predicting each of the volunteers

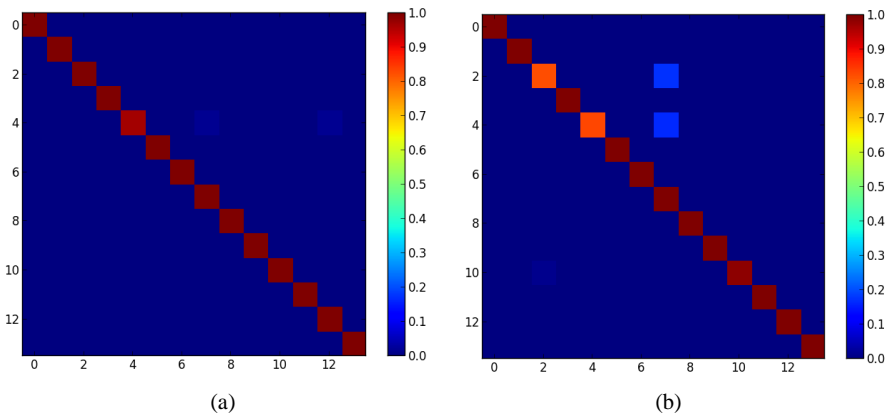| Volunteer	Nexus One		Optimus G		Volunteer	Nexus One		Optimus G	
	T	P	T	P		T	P	T	P
A	84	83	83	83	H	64	60	74	69
B	79	77	79	78	I	72	73	72	73
C	84	83	84	86	J	80	84	80	84
D	72	73	72	73	K	79	78	78	78
E	49	61	50	60	L	83	82	83	83
F	77	74	76	74	M	67	72	70	71
G	79	78	77	76	N	71	74	72	75

(a)   (b)

Fig. 5. Confusion matrices of the gait recognition on distinct samples extracted from the (a) Google Nexus One and (b) LG Optimus G phones

mus G is significantly higher than the Google Nexus One (100 Hz vs. 27 Hz). One main reason to interpret this phenomenon is the noises that were produced by the quality of the mobile sensor and the OS layer. The higher the sampling rate is, the noisier the product can be, which could negatively affect the gait recognition rate.

4.2 Impact of the sampling rate on extracted features

Table 4 illustrates the Average Error Rate (AER) and Intra-class Correlation Coefficients (ICC) of features extracted at the same time from both mobile devices. Most of the extracted features in the time domain (excepts avg_max_X, avg_min_X, $hist\_dist_X$), which had a low AER, showed that they were not under the influence of the sampling rate. Moreover, such features have excellent consistency with a high ICC ranging from 0.7 to 0.996 and hence, they can be extracted with a high reliability even when the sampling rate is totally different (32 Hz vs. 100 Hz).

Features in the frequency domain, including FFT, DCT coefficients have fair to good consistency with the ICC values ranging from 0.666 to 0.804. However, the AER ranging from 0.451 to 2.992 is rather high. Hence, they are very sensitive to the sampling rate. Such features

Table 4. The degree of agreements, including the AER and ICC, between features extracted from the Google Nexus One and LG Optimus G phones

Features	AER				ICC			
	X	**Y**	**Z**	**M**	**X**	**Y**	**Z**	**M**
avg_max	1.398	0.031	0.061	0.034	0.833	0.935	0.870	0.913
avg_min	0.898	0.152	1.413	0.104	0.749	0.905	0.835	0.928
avg_abs_diff	0.082	0.069	0.107	0.061	0.931	0.945	0.839	0.948
RMS	0.093	0.022	0.058	0.020	0.944	0.859	0.848	0.854
$hist\_dist$	0.869	0.451	0.473	0.408	0.705	0.740	0.595	0.672
σ	0.078	0.051	0.073	0.055	0.941	0.975	0.896	0.966
wl	0.143	0.107	0.093	0.085	0.904	0.948	0.902	0.951
T_{cad}	0.004				0.996			
f_{cad}	0.004				0.995			
fft	1.053	1.080	0.930	0.795	0.666	0.708	0.683,	0.678
dct	2.992	2.337	2.691	2.243	0.804	0.706	0.679	0.684

should be used with caution when building a cross-device for gait recognition.

4.3 Classification of the downsampling and upsampling rates

Figure 6 represents the classification accuracies of down/up-sampling the gait signals that have been acquired by both mobile devices with various sampling rates and levels of noise filtering. The best classification of each device is achieved at the sampling rate of 32 Hz and 36 Hz along with noise filtering at Level 2. Based on the characteristics of the wavelet decomposition technique, higher levels of decomposition will eliminate noise better. As discussed above, signals acquired by the Google Nexus One phone at a low frequency will contain less noise than the LG Optimus G device. Hence, using any level of decomposition (1, 2, and 3) at any sam-
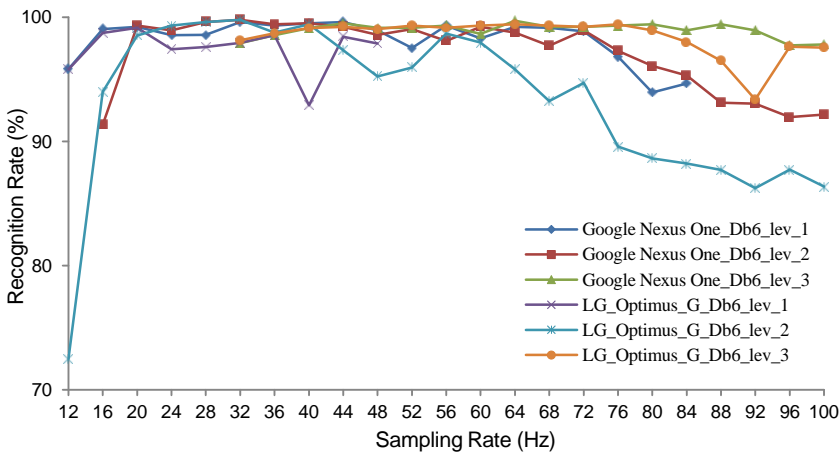

Fig. 6. Recognition rate at various sampling rates and the noise filtering level of both devices

pling rate does not significantly affect the accuracy rate.

In contrast to the Google Nexus One, the LG Optimus G produces more noises at the default sampling rate of 100 Hz. Hence, even when downsampling to a lower rate using linear interpolation, the noise is still high and as a result, the accuracy rate is reduced. Using noise filtering at Level 1 is only suitable for sampling rates ranging from 12 Hz to 48 Hz. With higher sampling rates, the noise not only decreases the accuracy rate but it will also harm the segmentation algorithm. Patterns extracted by using our algorithm do not reflect a sequence of gait cycles because too much noise prevents marking points from being vividly displayed. At Level 2, the segmentation algorithm could operate well at sampling rates ranging from 12 Hz to 100 Hz. However, the accuracy rate decrements significantly when the sampling rate increments, since this level is not enough to eliminate all noises at the high sampling rates. At the sampling rate of 100 Hz, the best accuracy rate of 97.53% is achieved by using wavelet decomposition (Daubechies of Level 6 in this study) at Level 3.

4.4 Cross-device gait recognition results

Based on results achieved from acquiring the down/up-sampling rate of both devices, we also did a cross-device experiment to check the possibility of deploying a unique gait recognition model on various devices. To do this, we synchronized the sampling rate of the Google Nexus One and the LG Optimus G to a fixed value. After that, samples extracted from the Google Nexus One were used to construct the classification model. Lastly, this model was used to predict samples extracted from the LG Optimus G. This process will reiterate vice versa in which, samples from the LG Optimus G are used to build up the classification model that was used to predict samples from the Google Nexus One. Moreover, based on the levels of the agreement of features extracted from both devices concurrently (Table 4), a poor level of agreement features (e.g. FFT, DCT coefficients, etc.) having a high AER or low ICC were excluded from the final feature vector to obtain the optimal set. Table 5 illustrates features that are kept to form the final feature vector, which is classified by SVM.

From our experiment, the most suitable value for the sampling rate is 36 Hz as it gives the best accuracy for a cross-device for gait recognition. Samples acquired by the Google Nexus One were used for training while samples from the LG Optimus G were used for prediction and vice versa and we achieved accuracy rates of 92.03 % and 90.68 %, respectively.

Table 5. Optimal features (marked as '×') used to construct a cross-device for gait recognition

Features	Axis				Features	Axis			
	X	Y	Z	M		X	Y	Z	M
avg_max		×	×	×	avg_abs_diff	×	×	×	×
avg_min		×		×	RMS		×		×
wl	×	×	×	×	$hist\_dist$		×		
					σ	×	×	×	×
T_{cad}	×				f_{cad}	×			

5. CONCLUSION

In this paper, we examined the impacts of the sampling rate on constructing an adaptive gait recognition model with two different mobile phones. The most suitable sampling rate of 32-36 Hz, with noise filtering at Level 2, was considered for constructing an effective gait recognition mechanism. This type of sampling rate is rather low, which could be very useful for saving energy on a mobile. Moreover, a cross-device for gait recognition was also discovered, based on analyzing the level of the agreements of extracted features. In this study, we only used interpolation as a simple method for down/up-sampling. Therefore, applying modern adjusting sampling rate techniques to improve the accuracy rate of a cross-device for gait recognition will be the main focus of further work that we need to conduct.

REFERENCES

[1] F. Breitinger and C. Nickel, "User Survey on Phone Security and Usage", in BIOSIG, Vol.164GI, 2010.

[2] K. Pousttchi and M. Schurig, "Assessment of today's mobile banking applications, from the view of customer requirements", in 37th HICSS'04, 2004.

[3] A. K. Jain, A. Ross and S. Prabhakar, "An Introduction to Biometric Recognition", in IEEE Transaction on Circuits and System for Video Technology, Vol.14, No.1, 2004.

[4] D. J. Fish and J. Nielsen, "Clinical assessment of human gait", in Journal of Prosthetics and Orthotics 2, April, 1993.

[5] S. Mondal, A. Nandy, P. Chakraborty and G.C Nandi, "Gait Based Personal Identification System Using Rotation Sensor", in CIS Journal, Vol.3, No.3, March, 2012.

[6] H. Sun and T. Yuao,"Curve Aligning approach for gait authentication based on a wearable sensor", in Physiological Measurement, Vol.33, No.6, May, 2012.

[7] L. Yuexiang, W. Xiabo, Q. Feng, "Gait Authentication Based on Acceleration Signals of Ankle", in Chinese Journal of Electronics, Vol.20, No.3 , July, 2011.

[8] S. Terada, Y. Enomoto, D. Hanawa and K. Oguchi, "Performance of gait authentication using an acceleration sensor", in 34th ICTSP, 2011.

[9] P. Bours and R. Shrestha, "Eigensteps: A giant leap for gait recognition", in IWSCN, May, 2010.

[10] D. Gafurov and E. Snekkenes, "Gait Recognition Using Wearable Motion Recording Sensors", in EURASIP Journal on Advances in Signal Processing, Vol.2009, 2009.

[11] G. Pan, Y. Zhang and Z. Wu, "Accelerometer-based gait recognition via voting by signature points", in IET Electronic Letters Vol.45, No.22, October, 2009.

[12] J. Mäntyjärvi, M. Lindholm, E. Vildjiounaite, S. M. Mäkelä, and H. Ailisto, "Identifying Users of Portable Devices From Gait Pattern With Accelerometers", in ICASSP, 2005.

[13] H. Ailisto, M. Lindholm, J. Mantyjarvi, E. Vildjounaite and S.M. Makela, "Identifying People from Gait Pattern with Accelerometers", in Proceeding of SPIE 5779, Biometric Technology for Human Identification II, April, 2005.

[14] H.M. Thang, V.Q. Viet, N. D. Thuc and D. Choi, "Gait Identification Using Accelerometer on Mobile Phone", in ICCAIS, 2012.

[15] M.R. Hestbek, C. Nickel and C. Busch, "Biometric Gait Recognition For Mobile Devices Using Wavelet Transform And Support Vector Machines", in IWSSIP 2012, April, 2012.

[16] C. Nickel and C. Busch,"Classifying Accelerometer Data via Hidden Markov Models to Authenticate People by the Way they Walk", in 2011 IEEE ICCST, October, 2011.

[17] C.Nickel, H. Brandt and C.Busch, "Classificatoin of Acceleration Data for Biometric Gait Recognition on Mobile Devices", in BIOSIG 2011, September, 2011.

[18] F. Frank, S. Mannor and D. Precup, "Activity and Gait Recognition with Time-Delay Embeddings", in 24th AAAI, 2010.

[19] M. O. Derawi, C. Nickel, P. Bours, and C. Busch, "Unobtrusive User-Authentication on Mobile Phones using Biometric Gait Recoginition", in 6th IIH-MSP, 2010.

[20] S. Sprager and D. Zazula, "A cumulant-based method for gait identification using accelerometer data with Principal Component Analysis and Support Vector Machine", in Journal WSEAS Transactions on Signal Processing, November, 2009.

[21] K. Holien, "Gait Recoginition under non-standard circumstances", Master thesis, Gjøvik University College, 2008.

[22] N. Kern, H. Junker, P. Lukowicz, B. Schiele and G. Troster, "Wearable Sensing to Annotate Meeting Recordings", in Journal Personal and Ubiquitous Computing, Vol.7, Issue 5, October, 2003, 2003.

[23] M. W. Whittle, "Gait analysis an introduction 4th edition", 2007.

[24] C. Chang and C.J. Lin, "LIBSVM: a library for support vector machines" in ACM Transactions on Intelligent Systems and Technology, 2011.

[25] J.M Bland and D.G Altman, "Statistical methods for assessing agreement between two metonds of clinical measurement", in The Lancet, Vol.327, Issue 8476, 1986.

[26] Koch and G. Gary, "Intraclass correlation coefficient", in Samuel Kotz and Norman L. Johnson. Encyclopedia of Statistical Sciences. 4. New York: John Wiley & Sons. pp.213-217, 1982.

[27] R. Senden, B. Grimm, I.C. Heyligers, H.H Savelberg and K. Meijer, "Acceleration-based gait test for healthy subjects: Reliability and reference data", in Gait Posture, 2009.

Thang Hoang

He received BS degree in Department of Computer Science, University of Science, VNU-HCMC in 2010. He is currently studying for his MS Degree in School of Electronics and Computer Engineering, Chonnam National University, South Korea. His research interests are context awareness, ubiquitous computing, mobile computing, biometrics, cryptography and pattern recognition.

Thuc Nguyen

He is Associate Professor of Knowledge Engineering Department at Faculty of Information Technology, University of Science, VNU-HCMC. He received BS degree in Faculty of Information Technology, University of Science, in 1990. He got PhD degree in University of Science, Vietnam in 2000. His interest on research spans from concrete structures and models, cryptography, database security and sensor network security.

Chuyen Luong

She received Engineering degree in School of Electronics and Telecommunications from Hanoi University of Sciences and Technology, Vietnam in 2012. She is currently studying for her MS Degree in School of Electronics and Computer Engineering, Chonnam National University, South Korea. Her research interests are mainly in the field of context awareness, pattern recognition

Son Do

He received BS degree in Department of Math and Computer Science, University of Science, VNU-HCMC in 2011. He is currently studying for his MS Degree in School of Electronics and Computer Engineering, Chonnam National University, South Korea. His research interests are context awareness, and pattern recognition.

Deokjai Choi

He is full professor of Computer Engineering Department at Chonnam National University, South of Korea. He received BS degree in Department of Computer Science, Seoul National University, in 1982. He got MS degree in Department of Computer Science, KAIST, South Korea in 1984. He got PhD degree in Department of Computer Science and Telecommunications, University of Missouri-Kansas City, USA in 1995. His interest on research spans from context awareness, pervasive computing, sensor network, future Internet and IPv6.